

Paper-Based Microfluidic Device with Integrated Sputtered Electrodes for Stripping Voltammetric Determination of DNA via Quantum Dot Labeling

Christos T. Kokkinos,^{*,†} Dimosthenis L. Giokas,^{‡,§} Anastasios S. Economou,^{*,†,§} Panagiota S. Petrou,[§] and Sotirios E. Kakabakos[§]

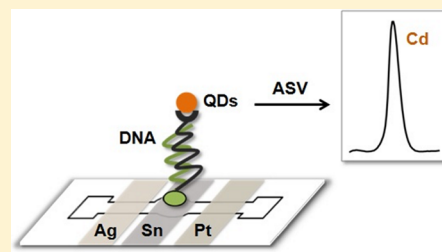
[†]Laboratory of Analytical Chemistry, Department of Chemistry, University of Athens, Athens 15771, Greece

[‡]Laboratory of Analytical Chemistry, Department of Chemistry, University of Ioannina, Ioannina 45110, Greece

[§]Immunoassays/Immunosensors Lab, INRaSTES, NCSR “Demokritos”, Aghia Paraskevi, 15310, Greece

Supporting Information

ABSTRACT: This work reports a microfabricated electrochemical paper-based analytical device (ePAD) for the voltammetric determination of DNA. The device is patterned by wax-printing on paper and features a circular assay zone connected to an inlet zone and a sink via grooved microfluidic channels for accelerated flow rate. An electrochemical cell with integrated electrodes is formed on the reverse side of the paper by sputtering of thin metal films (Sn, Pt and Ag as the working, counter and reference electrode, respectively). Proof-of-principle of the ePAD for biosensing is demonstrated for a DNA assay involving attachment of capture DNA, hybridization with biotinylated target oligonucleotide and labeling with streptavidin-conjugated CdSe/ZnS quantum dots (QDs). After the acidic dissolution of the QDs, the released Cd(II) is quantified by anodic stripping voltammetry (ASV) at the Sn-film working electrode. Thanks to the synergistic effects of QDs amplification, the inherent sensitivity of ASV and the excellent detection capabilities of the Sn-film working electrode for Cd(II), the target DNA can be detected at levels as low as 0.11 pmol L⁻¹ using sample volumes as low as 1 μL. The developed microfluidic ePAD costs only 0.11\$ and presents favorable fabrication and operational features that make it an excellent candidate biosensor for simple and ultrasensitive point-of-need testing.



Assays for the selective, sensitive, fast, and low-cost determination of important biomolecules (proteins and DNA) play an important role in modern diagnostics.^{1–3} Over the last years, flexible substrates, such as polymers and paper, have been increasingly used for the development of bioanalytical devices.^{2–8}

Paper is a very attractive substrate for the development of biosensors being flexible, widely available, inexpensive, and hydrophilic. Its surface can be easily modified or patterned and exhibits strong adsorptive properties for biomolecules and nanoparticles (NPs). In addition, paper is safe, easy to dispose of, and biocompatible. Finally, one of the main attractions of cellulose is its porosity which allows solution transport through capillary forces, thus serving as an autonomous microfluidic pumping system without the requirement of external pumps.^{4–8}

Electrochemical detection is well suited to paper-based analytical devices (PADs) since electrodes can be miniaturized and easily deposited onto paper using various technologies. Electrochemical detectors are also inexpensive and portable with negligible power consumption, and the wide variety of available detection formats provides flexibility in the selection of the biochemical assay protocols.^{4–8} Various electrochemical PADs (ePADs) have been reported for biosensing.^{9–20}

Reflecting the significant progress in the field of nanotechnology and nanomaterials, ultrasensitive bioassays have been developed using labeling of biomolecules with noble metal (Au or Ag) NPs or quantum dots (QDs) (nanocrystals consisting of sulfide or selenide salts of heavy metals such as Cd, Pb, or Zn).^{3,21–23} Chemical oxidation of these nanolabels results in the release of metal cations that can be detected with great sensitivity by anodic stripping voltammetry (ASV).^{2,3} When this detection format is applied to integrated biosensors (and for that matter to ePADs), some of the most critical challenges are associated with the working electrode (i.e., choice of material, method of deposition on the substrate, and miniaturization aspects).^{2,3} Our group has pioneered the fabrication of “green” (bismuth and tin) electrodes via microengineering approaches (such as sputtering) and their application to heavy metal analysis.^{24–26} Recently, we have also demonstrated that such microfabricated electrodes can be deposited on flexible substrates and used in conjunction with QDs for bioassays.²⁷

However, despite its many attractions for biosensing, the area of ePADs using NPs or QDs labels and ASV detection still

Received: October 17, 2017

Accepted: December 18, 2017

Published: December 18, 2017

remains largely unexplored. Only two folding (origami) ePADs have been recently described for biosensing of ricin and DNA using bioconjugated magnetic beads as preconcentration moieties, AgNPs as voltammetric labels and printed carbon electrodes.^{19,20} Although PADs with optical detection have been recently described for QD-based immunoassays,^{28,29} so far there are no reports of ePADs using QD labels for bioassays. Regarding electrochemical DNA detection with PADs, except from the origami ePAD mentioned above,¹⁹ only a few reports exist in the pertinent literature using enzymatic or redox labels,^{14–18} often combined with signal amplification strategies based on the modification of printed carbon working electrodes with Au particles and/or graphene.^{16–18}

In this work, we describe a simple integrated microfluidic ePAD for drop-volume bioassays based on ASV detection of Cd-based QDs labels. The device is composed of (i) a wax-printed circular assay zone connected to inlet zone and a sink via grooved microfluidic channels for accelerated fluid transport rate and (ii) a voltammetric cell formed on the reverse side of the paper substrate featuring sputtered thin films of Sn as a working electrode (WE), Ag as a reference electrode (RE), and Pt as a counter electrode (CE). Proof-of-principle of the microfluidic ePAD for biosensing is demonstrated for the quantitative assay of the DNA mutation related to the Multiple Endocrine Neoplasia Type 2. The QD-based DNA assay is implemented by attachment of capture DNA in the assay zone, hybridization with biotinylated target oligonucleotide, and labeling with streptavidin-conjugated CdSe/ZnS quantum dots (STV-CdSe/ZnS QDs). After the acidic dissolution of the QDs, the released Cd(II) is quantified by square wave anodic stripping voltammetry (SWASV) at the Sn-film WE (Scheme 1). The ePAD offers a limit of detection (LOD) at

subpicomolar levels without using any extra signal amplification step (i.e., magnetic beads or electrode modification) demonstrating several advantages, in terms of fabrication and operational features, compared with existing electrochemical DNA biosensors.

EXPERIMENTAL SECTION

Reagents and Apparatus. The reagents and apparatus used are described in detail in the [Supporting Information](#).

Fabrication of the ePADs. The fabrication process of the ePADs is illustrated in [Figure 1A](#), and photographs of the

Scheme 1. Schematic Presentation of the Preparation of Paper-Based Biosensor, the QD-Based DNA Assay, and the Detection by ASV

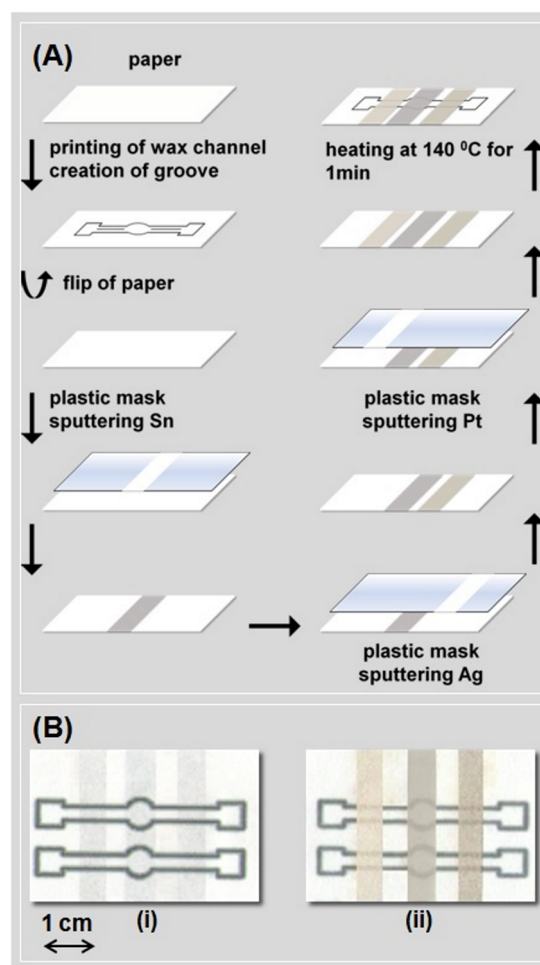
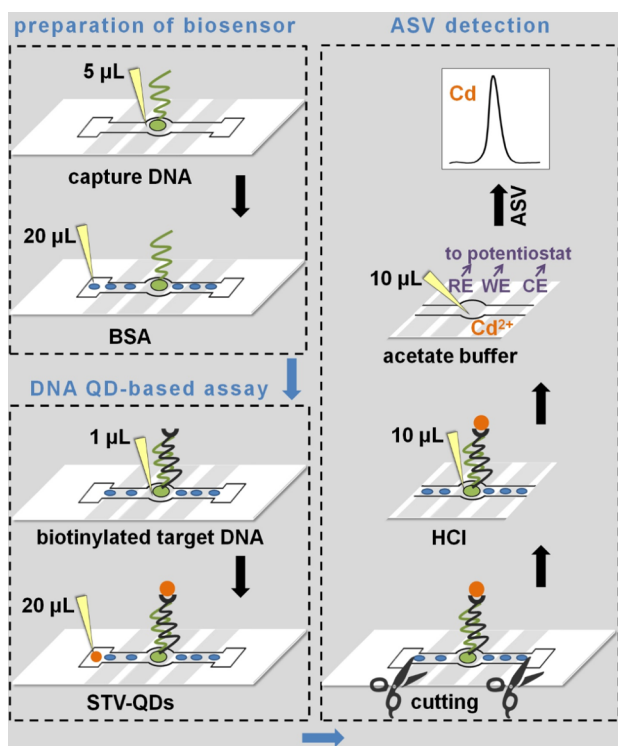


Figure 1. (A) Schematic procedure of the fabrication of the microfluidic ePADs and (B) photographs of the ePADs: (i) front and (ii) back face.

device are shown in [Figure 1B](#). Initially, the microfluidic pattern (channels, inlet and assay zones, and sink) was wax-printed on the paper substrate. The detailed dimensions of the microfluidic channels are shown in [Figure S1](#) of the [Supporting Information](#). The channels were engraved using a line plotter (Linear 1200, Barnstead International) equipped with a precision knife with a Chisel-type grind; the average width of the grooves was $135 \pm 15 \mu\text{m}$. Next, the sputtering process was performed on the reverse side of paper substrate, using three polyester sheets (Mac Dermid) as pattern masks. Each mask has a slot (4 mm in width) for the deposition of the respective electrode on the paper surface. The three electrodes were deposited by successively sputtering each metal on paper in the following

order: Sn (400 nm, power of 40 W), Ag (400 nm, constant current of 25 mA), and Pt (400 nm, power of 30 W), each time using the specific mask. Finally, the ePAD was placed in an oven for 1 min at 140 °C so that the wax melted and penetrated the paper, creating the hydrophobic barriers defining the microfluidic channels. At the lab scale, 72 devices were simultaneously produced in every fabrication run.

Preparation of the Biosensor. For the preparation of biosensor, 5 μL of a 5.0 $\mu\text{g mL}^{-1}$ solution of BSA-capture DNA conjugate in phosphate buffer saline (PBS) (50 mmol L^{-1} , pH 7.4) was placed in the circular assay zone of the ePAD and was left to dry at ambient conditions. After the immobilization of the capture oligonucleotide, the free sites of the channel were blocked by adding 20 μL of blocking solution (3% (w/v) BSA in 20 mmol L^{-1} PBS, pH 7.0, containing 0.05% (v/v) Tween 20) in the inlet zone and the ePAD was left to dry at ambient conditions (Scheme 1).

DNA QD-Based Assay. The workflow of the assay is illustrated in Scheme 1. A portion of 1 μL of the biotinylated target DNA solution in 1 \times HEN (0.10 mol L^{-1} HEPES, 0.0050 mol L^{-1} NaCl, 1.0 mmol L^{-1} EDTA, pH 8.0) was added to the circular assay zone and incubated until the device dried at ambient conditions. After hybridization with the capture DNA, the biosensor was washed by adding 2 \times 20 μL of 1 \times HEN buffer in the inlet zone. Then, 20 μL of a 10.0 nmol L^{-1} solution of STV-CdSe/ZnS QDs in 1 \times HEN was added in the inlet zone, transported to the circular assay zone by capillary action, and allowed to react with the target DNA until the device dried. Then, the ePAD was washed by adding 2 \times 20 μL of 1 \times HEN buffer in the inlet zone and was left to dry. Finally, after the assay, the inlet zone and the sink were cut off the device using scissors. For the discrimination experiments, the ePAD was sequentially washed with 20 μL of HEN buffers (from 1 \times HEN to 0.0625 \times HEN) and finally with 20 μL of distilled water.

Detection by ASV. Following the DNA hybridization assay, 10 μL of 0.010 mol L^{-1} HCl solution was added in the circular assay zone and left for 10 min to oxidize the QDs and to release Cd(II). Then, 10 μL of 0.10 mol L^{-1} acetate buffer (pH 4.5) was added in the circular assay zone. Preconcentration of Cd(II) was carried out at the Sn-film WE at -1.20 V for 120 s. Then, the potential of the WE was scanned in the range -0.95 to -0.65 V in the SW mode (frequency, 50 Hz; pulse height, 40 mV; step increment, 4 mV) in order to record the Cd stripping peak.

RESULTS AND DISCUSSION

Design and Fabrication Features of the ePAD. The microfluidic ePAD is designed to address the limitations associated with existing QD-based DNA assays with ASV detection such as the need for handling large volumes of solutions and samples, the use of large-sized electrodes, the requirement for stirring, and the lack of portability and disposability.^{24,30–42}

The two ePADs reported for biosensing through ASV detection of AgNPs labels make use of magnetic beads as amplifiers and are based on the origami (folding paper) format which inevitably complicates the design, the fabrication, and the operation of the devices.^{19,20} In this work, we have decided to use a 2D (planar) microfluidic lateral flow configuration which results in a very simple device in terms of design, fabrication, and operation. Wax-printing is chosen to define the microfluidic channels, the assay and inlet zone, and the sink since this

is a simple and cost-effective micropatterning method.⁸ The device consists of two rectangular zones (inlet zone for addition of reagents and sink for the collection of the waste) connected to one circular assay zone via two equally sized microfluidic channels. The Sn-film WE is deposited on the reverse side of the paper just underneath the assay zone in such a way as to be in direct spatial contact with the solution in the assay zone (Figure 1). A critical feature of the device is the engraving of the microfluidic channels in order to accelerate the fluid transport from the inlet zone to the assay zone, thanks to a laminar flow regime as demonstrated in previous work.⁴³ Two different configurations of engraving were tested, one with a single continuous groove along the inlet channel and another with two dashed grooves (Figure S1 of the Supporting Information). In the configuration employing a single groove, the fluid delivery time to the assay zone decreased by approximately 60%, as opposed to a 35% reduction obtained with the dashed grooves; thus, a single channel was used in the final design (Figure S1 of the Supporting Information).

In addition, in an effort to increase the sensitivity, to simplify the assay workflow, and to produce ready-to-use ePADs, we have decided to exploit labeling with Cd-based QDs (rather than metal NPs) and to adopt sputtered metal-film electrodes (instead of bare carbon electrodes). It has been demonstrated that QDs labels provide enhanced detection sensitivity and increase the scope for multiplexing compared to metal NPs labels.^{2,3,21,22} Besides, the detection sensitivity for heavy metal cations (Pb(II), Cd(II), Zn(II)) released from QDs can be substantially enhanced by modifying carbon electrodes with a thin film of an alloy-forming metal (mercury, bismuth, tin), typically by electroplating.^{44–46} An alternative approach is patterning of electrodes by sputtering thin films of alloy-forming metals on a suitable substrate; this fabrication method provides flexibility in defining the electrode geometry and thickness, ensures strictly reproducible fabrication conditions, and enables mass-fabrication of sensors.^{24–27} Among the candidate electrode materials, mercury is toxic and, being liquid, cannot be patterned by sputtering. On the other hand, bismuth and tin are “greener” alternatives to mercury for heavy metal detection and can be readily deposited by sputtering.^{24–27} A sputtered Sn-film WE offered nearly a 2-fold enhancement in sensitivity for Cd(II) detection compared to a sputtered Bi-film WE (Figure S2 of the Supporting Information). Therefore, a Sn-film was selected as the WE material while Ag and Pt thin films were used as the RE and CE, respectively. The operational potential window of the Sn-film WE was studied by DC voltammetry by scanning the potential in the range from -1.40 to -0.40 V in 0.1 mol L^{-1} acetate buffer (pH 4.5) (Figure S3 of the Supporting Information). A flat polarization curve was obtained in the range from -1.25 to -0.60 V. At potentials more negative than -1.25 V, the reduction of hydroxonium ions took place, while at potentials more positive than -0.60 V the Sn started to oxidize. These results prove that the sputtered Sn-film is a suitable WE for SWASV determination of Cd(II).

The three metallic films on the ePAD presented satisfactory adhesion to the paper substrate without the need for any extra buffer layer. As illustrated in the FESEM image in Figure 2A, Sn deposition by sputtering resulted in uniform coverage of the paper substrate with the metal film, with the characteristic granular structure of sputtered Sn.²⁴ The thickness of the Sn-film WE was examined in the range of 200–600 nm (in 200 nm steps) by varying the duration of the deposition step. The Sn

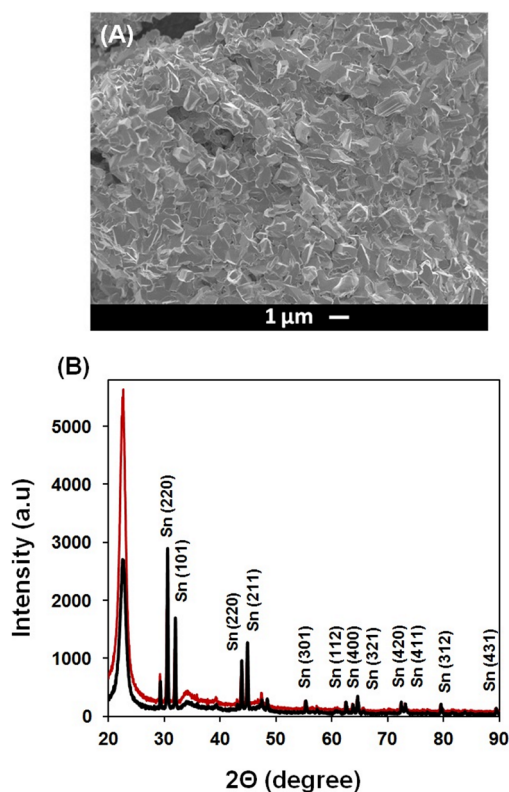


Figure 2. (A) FESEM image of the Sn-film WE surface and (B) XRD spectra of the Sn-film WE surface on the ePAD (black line) and of the plain paper surface (red line).

film with 200 nm thickness yielded lower stability and lifetime, while Sn films 400 nm- and 600 nm-thick provided similar results for Cd(II) detection; a 400 nm-thick Sn film was used as the WE in the final design. In the XRD spectrum of the Sn film, the numerous specific peaks suggested polycrystalline Sn deposition. The additional peaks in the XRD spectrum stem from the paper substrate, while no further peaks appeared, showing that no oxidation of Sn took place during the sputtering deposition procedure (Figure 2B).

DNA QD-Based Assay. The selected protocol for the DNA assay involves formation of a triple bioconjugate of capture DNA/biotinylated target DNA/STV-modified QDs instead of the more conventional sandwich assay using a QD-labeled probe DNA as the third component of the bioconjugate. Sandwich assays require the preparation of dedicated oligonucleotide–QD conjugates for each different target DNA as well as the implementation of two hybridization events of target DNA with capture oligonucleotide and with oligonucleotide–QDs conjugate.^{32,33,35,37,39} On the other hand, the STV-conjugated QDs provide higher flexibility, since they can be used to label any biotinylated target DNA and thus, the scope of the developed assay could be extended to the detection of different target DNA. Finally, the use of STV-conjugated QDs makes the assay directly applicable to DNA detection after PCR since biotinylated oligonucleotides can be directly produced using specific biotinylated primers.^{47,48}

In order to reduce the signal of the nonspecific binding, different experiments were carried out: (i) various concentrations of blocking BSA solutions ranging from 1.0 to 4.0% (w/v) in 20 mmol L⁻¹ PBS, pH 7.0, or in 0.10 mol L⁻¹ carbonate buffer, pH 8.5, with or without 0.05% (v/v) Tween

20, were examined; 3% (w/v) BSA in PBS containing Tween 20 was selected and (ii) addition of the STV-conjugated QDs solution was performed either directly in the circular assay zone or in the inlet zone and the latter approach was adopted. In order to reduce the respective volumes, the capture oligonucleotide solution and the DNA sample were directly added to the circular assay zone where the hybridization event takes place.

Analytical Characteristics of the ePAD. The analytical characteristics of the presented microfluidic ePAD for the QD-based DNA voltammetric assay were assessed by carrying out the assay with different concentrations of target DNA ranging from 0.50 pmol L⁻¹ to 50 nmol L⁻¹. The stripping peak height of Cd(II) (released from QDs) was linearly related to the logarithm of the target oligonucleotide concentration (Figure 3A,B). The regression equation was

$$I(\mu\text{A}) = (4.0 \pm 0.2) \times \log[\text{DNA}](\text{mol L}^{-1}) + (54 \pm 2), \\ R^2 = 0.993 (n = 5)$$

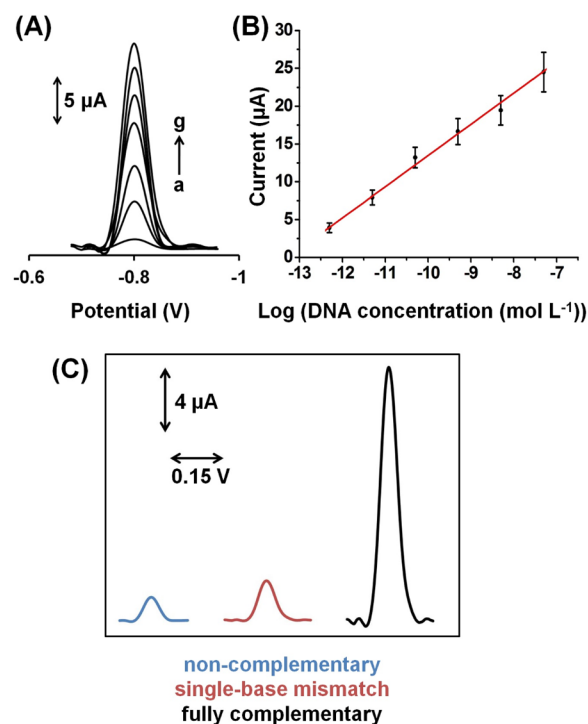


Figure 3. (A) Baseline-corrected SWASV voltammograms obtained with the microfluidic ePADs for target DNA concentrations: 0, 0.50, 5.0, and 50 pmol L⁻¹, 0.50, 5.0, and 50 nmol L⁻¹ from (a) to (g). (B) The respective calibration plot for the target DNA in the range from 0.50 pmol L⁻¹ to 50 nmol L⁻¹. The points are the mean value \pm sd ($n = 5$) subtracting the mean signal of the blank (0 pmol L⁻¹ target DNA). (C) Baseline-corrected SWASV voltammograms for: 0.50 nmol L⁻¹ of noncomplementary, single-base mismatch and fully complementary sequences. Conditions as in text.

The LOD was 0.11 pmol L⁻¹ (equivalent to 0.11 amol in the 1 μ L DNA sample) and was estimated as the concentration of target DNA corresponding to three times the standard deviation of the blank sample. The LOD for DNA using the proposed microfluidic ePAD is comparable to, or lower than, other QD-ASV DNA assays using conventional electroplated electrodes (ranging from 0.24 pmol L⁻¹ to 1.5 μ mol

L^{-1}).^{32,33,37–41} It is also significantly lower than ePADs for DNA determination employing either magnetic beads, electrode modifiers, or enzymatic labeling (ranging from 85 pmol L^{-1} to 30 nmol L^{-1}).^{19,15–17} It is important to note that this excellent LOD was achieved without any additional amplification approach (e.g., use of magnetic beads or modification of the electrode).

The between-sensor reproducibility (expressed as the % RSD of the Cd stripping signal for the detection of 20 $\mu g L^{-1}$ Cd(II) at 5 different ePADs) was 4.8%, indicating satisfactory fabrication reproducibility. The between-bioassay reproducibility (in terms of the % RSD of five independent bioassays) ranged from 10.1 to 13.2% over the whole DNA calibration range (0.50 pmol L^{-1} to 50 nmol L^{-1}) (Figure S4 of the Supporting Information). The ePADs, after modification with capture DNA, blocking with BSA, and drying under nitrogen, were kept in sealed boxes at 4 °C. After 4 weeks of storage, a *t*-test demonstrated that the ASV response of the biosensor remained statistically stable (Figure S5 of the Supporting Information).

The selectivity of the DNA ePADs was assessed against noncomplementary and single-base mismatch sequences, respectively (Figure 3C). The response of the fully complementary target sequence was 12.6 (± 1.4) times higher than that of the single-base mismatch sequence. The peak height of the noncomplementary sequence was comparable with that of the blank response (0 pmol L^{-1} target DNA). Thus, the selectivity was satisfactory and comparable or better than other electrochemical QD-ASV DNA assays.^{24,27,34,35,38,41,42} These results provide evidence that the proposed ePADs are able to provide DNA detection with high sensitivity and selectivity.

Finally, the cost of each ePAD was calculated at \$0.11 at our lab scale in which 72 devices were simultaneously produced (bill of materials per ePAD, \$0.0087 for Whatman Chr 1 paper, \$0.0002 for wax-printing, \$0.0076 for tin sputtering, \$0.0229 for silver sputtering, \$0.0719 for platinum sputtering).

CONCLUSIONS AND OUTLOOK

In this work, a new type of microfluidic ePAD with integrated sputtered metal-film electrodes is described for the ultrasensitive voltammetric assay of DNA employing Cd-based QDs as labels. In addition to the well documented advantages of PADs, the particular device (a) can function with only tiny volumes of sample (as low as 1 μL), (b) has extended scope for mass-production (even at lab scale 72 ePADs can be simultaneously fabricated), (c) is extremely low cost (each ePAD costs only \$0.11), (d) can achieve subpicomolar LODs by exploiting the combination of labeling with QDs, ASV detection, and a Sn-film WE without any additional signal amplification step, (e) provides high flexibility by using STV-conjugated QDs which can be used to label different biotinylated target biomolecules. Finally, the ePAD is suitable for the simultaneous determination of Cd(II) and Zn(II) by ASV (Figure S6 of the Supporting Information) and thus, the applicability of the proposed device can be extended to duplex voltammetric biosensing. The main disadvantage of the ePAD is the limited temporal control over the different steps of the assay (since the timing of each step is dictated by the time it takes for the ePAD to dry).

ASSOCIATED CONTENT

Supporting Information

The Supporting Information is available free of charge on the ACS Publications website at DOI: 10.1021/acs.analchem.7b04274.

Reagents and apparatus, fluid delivery time at the microfluidic grooved channels, comparison between sputtered bismuth and sputtered tin film electrodes for ASV of Cd(II), polarization range of the Sn-film working electrode, between-sensor and between-bioassay reproducibility, stability of the microfluidic ePADs, and simultaneous ASV determination of Cd(II) and Zn(II) at the ePAD (PDF)

AUTHOR INFORMATION

Corresponding Authors

*E-mail: xxokkinos@gmail.com; christok@chem.uoa.gr. Phone: +306972937675.

*E-mail: aeconomou@chem.uoa.gr. Phone: +302107274298.

ORCID

Dimosthenis L. Giokas: 0000-0002-1816-5810

Anastasios S. Economou: 0000-0003-4590-9261

Notes

The authors declare no competing financial interest.

ACKNOWLEDGMENTS

The research project was implemented under the IKY Scholarship which was funded by the Action “Strengthening Postdoctoral Researchers” act from the resources of EP “Human Resources Development Program, Education and Lifelong Learning” with priority axes 6,8,9 and is cofinanced by the European Social Fund (ESF) and the Greek Government.

REFERENCES

- (1) Liu, A.; Wang, K.; Weng, S.; Lei, Y.; Lin, L.; Chen, W.; Lin, X.; Chen, Y. *TrAC, Trends Anal. Chem.* **2012**, *37*, 101–111.
- (2) Kokkinos, C.; Economou, A.; Prodromidis, M. I. *TrAC, Trends Anal. Chem.* **2016**, *79*, 88–105.
- (3) Kokkinos, C.; Economou, A. *Anal. Chim. Acta* **2017**, *961*, 12–32.
- (4) Desmet, C.; Marquette, C. A.; Blum, L. J.; Doumeche, B. *Biosens. Bioelectron.* **2016**, *76*, 145–163.
- (5) Marzo, A. M. L.; Merkoci, A. *Lab Chip* **2016**, *16*, 3150–3176.
- (6) Mettakoonpitak, J.; Boehle, K.; Nantaphol, S.; Teengam, P.; Adkins, J. A.; Srisa-Art, M.; Henry, C. S. *Electroanalysis* **2016**, *28*, 1420–1436.
- (7) Yang, Y.; Noviana, E.; Nguyen, M. P.; Geiss, B. J.; Dandy, D. S.; Henry, C. S. *Anal. Chem.* **2017**, *89*, 71–91.
- (8) Xia, Y.; Si, J.; Li, Z. *Biosens. Bioelectron.* **2016**, *77*, 774–789.
- (9) Nunez-Bajo, E.; Blanco-Lopez, M. C.; Costa-Garcia, A.; Fernandez-Abedul, M. T. *Biosens. Bioelectron.* **2017**, *91*, 824–832.
- (10) Nantaphol, S.; Chailapakul, O.; Siangproh, W. *Anal. Chim. Acta* **2015**, *891*, 136–143.
- (11) Wu, Y.; Xue, P.; Hui, K. M.; Kang, Y. *Biosens. Bioelectron.* **2014**, *52*, 180–187.
- (12) Cao, L.; Fang, C.; Zeng, R.; Zhao, X.; Jiang, Y.; Chen, Z. *Biosens. Bioelectron.* **2017**, *92*, 87–94.
- (13) Ge, S.; Zhang, L.; Zhang, Y.; Liu, H.; Huang, J.; Yan, M.; Yu, J. *Talanta* **2015**, *145*, 12–19.
- (14) Wang, Y.; Ge, L.; Ma, C.; Kong, Q.; Yan, M.; Ge, S.; Yu, J. *Chem. - Eur. J.* **2014**, *20*, 12453–12462.
- (15) Tian, T.; Liu, H.; Li, L.; Yu, J.; Ge, S.; Song, X.; Yan, M. *Sens. Actuators, B* **2017**, *251*, 440–445.
- (16) Teengam, P.; Siangproh, W.; Tuantranont, A.; Henry, C. S.; Vilaivan, T.; Chailapakul, O. *Anal. Chim. Acta* **2017**, *952*, 32–40.

- (17) Cunningham, J. C.; Brenes, N. J.; Crooks, R. M. *Anal. Chem.* **2014**, *86*, 6166–6170.
- (18) Lu, J.; Ge, S.; Ge, L.; Yan, M.; Yu, J. *Electrochim. Acta* **2012**, *80*, 334–341.
- (19) Li, X.; Scida, K.; Crooks, R. M. *Anal. Chem.* **2015**, *87*, 9009–9015.
- (20) Cunningham, J. C.; Scida, K.; Kogan, M. R.; Wang, B.; Ellington, A. D.; Crooks, R. M. *Lab Chip* **2015**, *15*, 3707–3715.
- (21) Valera, E.; Albors, A. H.; Marco, M. P. *TrAC, Trends Anal. Chem.* **2016**, *79*, 9–22.
- (22) Wu, L.; Xiong, E.; Zhang, X.; Zhang, X.; Chen, J. *Nano Today* **2014**, *9*, 197–211.
- (23) Shu, J.; Tang, D. *Chem. - Asian J.* **2017**, *12*, 2780–2789.
- (24) Kokkinos, C.; Economou, A.; Petrou, P. S.; Kakabakos, S. E. *Anal. Chem.* **2013**, *85*, 10686–10691.
- (25) Kokkinos, C.; Economou, A. *Talanta* **2014**, *125*, 215–220.
- (26) Kokkinos, C.; Economou, A. *Sens. Actuators, B* **2016**, *229*, 362–369.
- (27) Kokkinos, C.; Economou, A.; Speliotis, T.; Petrou, P. S.; Kakabakos, S. E. *Anal. Chem.* **2015**, *87*, 853–857.
- (28) Lin, Z.; Lv, S.; Zhang, K.; Tang, D. *J. Mater. Chem. B* **2017**, *5*, 826–833.
- (29) Qiu, Z.; Shu, J.; Tang, D. *Anal. Chem.* **2017**, *89*, 5152–5160.
- (30) Moulick, A.; Milosavljevic, V.; Vlachova, J.; Podgajny, R.; Hynek, D.; Kopel, P.; Adam, V. *Int. J. Nanomed.* **2017**, *12*, 1277–1291.
- (31) Krejčová, L.; Huska, D.; Hynek, D.; Kopel, P.; Adam, V.; Hubalek, J.; Trnkova, L.; Kizek, R. *Int. J. Electrochem. Sci.* **2013**, *8*, 689–702.
- (32) Sun, A. L.; Zhang, Y. F.; Wang, X. N. *Microchim. Acta* **2015**, *182*, 1403–1410.
- (33) Wang, J.; Liu, G. D.; Jan, M. R.; Zhu, Q. *Electrochem. Commun.* **2003**, *5*, 1000–1004.
- (34) Dong, H.; Yan, F.; Ji, H.; Wong, D. K.; Ju, H. *Adv. Funct. Mater.* **2010**, *20*, 1173–1179.
- (35) Xiang, Y.; Zhang, H.; Jiang, B.; Chai, Y.; Yuan, R. *Anal. Chem.* **2011**, *83*, 4302–4306.
- (36) Baek, S.; Won, B. Y.; Park, K. S.; Park, H. G. *Biosens. Bioelectron.* **2013**, *49*, 542–546.
- (37) Wang, J.; Liu, G.; Merkoci, A. *J. Am. Chem. Soc.* **2003**, *125*, 3214–3215.
- (38) Yang, T.; Huang, D.; Li, Q.; Zhang, W.; Jiao, K. *Electroanalysis* **2012**, *24*, 392–397.
- (39) Jie, G.; Zhang, J.; Jie, G.; Wang, L. *Biosens. Bioelectron.* **2014**, *52*, 69–75.
- (40) Huang, H.; Li, J.; Tan, Y.; Zhou, J.; Zhu, J. J. *Analyst* **2010**, *135*, 1773–1778.
- (41) Marin, S.; Merkoci, A. *Nanotechnology* **2009**, *20*, 055101.
- (42) Kokkinos, C.; Prodromidis, M.; Economou, A.; Petrou, P. S.; Kakabakos, S. E. *Electrochem. Commun.* **2015**, *60*, 47–51.
- (43) Giokas, D. L.; Tsogas, G. Z.; Vlessidis, A. G. *Anal. Chem.* **2014**, *86*, 6202–6207.
- (44) Economou, A.; Fielden, P. R. *Analyst* **2003**, *128*, 205–213.
- (45) Kokkinos, C.; Economou, A. *Curr. Anal. Chem.* **2008**, *4*, 183–190.
- (46) Alves, G. M. S.; Rocha, L. S.; Soares, H.M.V.M. *Talanta* **2017**, *175*, 53–68.
- (47) Campuzano, S.; Pedrero, M.; Garcia, J. L.; Garcia, E.; Garcia, P.; Pingarron, J. M. *Anal. Bioanal. Chem.* **2011**, *399*, 2413–2420.
- (48) Kalogianni, D. P.; Boutsika, L. M.; Kouremenou, P. G.; Christopoulos, T. K.; Ioannou, P. C. *Anal. Bioanal. Chem.* **2011**, *400*, 1145–1152.